Available online at www.sciencedirect.com
SCIENCE DIRECT®
International Journal of Thermal Sciences 42 (2003) 283–293
International Journal of Thermal Sciences
www.elsevier.com/locate/ijts

Mixed convection boundary layer flow about an isothermal sphere in a micropolar fluid

Roslinda Nazar [a], Norsarahaida Amin [a], Ioan Pop [b,*]

[a] *Department of Mathematics, Universiti Teknologi Malaysia, 81310 Johor Bahru, Johor, Malaysia*
[b] *Faculty of Mathematics, University of Cluj, R-3400 Cluj, CP 253, Romania*

Received 18 February 2002; accepted 4 April 2002

Abstract

The steady mixed convection boundary layer flow of a micropolar fluid about a sphere with a constant surface temperature is considered for both the assisting and opposing flow cases. The transformed conservation equations of the non-similar boundary layers are solved numerically using a very efficient finite-difference method known as the Keller-box scheme. Numerical results are presented for different values of the material and mixed convection parameters K and λ, respectively, and with the Prandtl number $Pr = 0.7$ and 7. It is found that assisting flow ($\lambda > 0$) delays separation of the boundary layer and can, if the assisting flow is strong enough, suppress it completely. The opposing flow ($\lambda < 0$), on the other hand, brings the separation point nearer to the lower stagnation point of the sphere and for sufficiently strong opposing flows there will not be a boundary layer on the sphere. Some results were given in the form of tables. Such tables are very important and they can serve as a reference against which other exact or approximate solutions can be compared in the future.

Keywords: Micropolar fluid; Mixed convection; Boundary layer; Isothermal sphere; Numerical results

1. Introduction

The theory of micropolar fluids proposed by Eringen [1, 2] deals with the class of fluids which exhibit certain microscopic effects arising from the local structure of the micromotions of the fluid elements. This theory has recently received considerable attention because of its applications in a number of processes that occur in industry. Such applications include the extrusion of polymer liquids, solidification of liquid crystals, cooling of a metallic plate in a bath, ferro liquids, etc. Physically, the micropolar fluid can consist of a suspension of small rigid cylindrical elements such as large dumbbell-shaped molecules. The theory of micropolar fluid is generating a very much increased interest and many classical flows are being re-examined to determine the effects of the fluid microstructure. A detailed review made by Ariman et al. [3] and the recent papers by Gorla [4], Gorla et al. [5], Bhattacharyya and Pop [6], Hossain and Chowdhury [7], Rees and Bassom [8], Rees and Pop [9], Hossain et al. [10–12] and Nazar et al. [13–15] clearly show the fast development of the theory of the micropolar fluid.

Of more interest to the present work are the papers by Lien and Chen [16] who have studied the steady mixed convection boundary layer flow of a micropolar fluid about a permeable sphere and Wang and Kleinstreuer [17] who generalized the paper by Lien and Chen [16] to two-dimensional axisymmetric bodies with porous walls and constant surface temperature or heat flux. Lien and Chen [16] have used the Mangler transformation and potential outer flow velocity, while Wang and Kleinstreuer [17] have introduced a new coordinate transformation to reduce the streamwise dependence in the coupled boundary layer equations. However, these authors have introduced three material parameters.

The purpose of this paper is to analyze the steady mixed convection boundary layer flow of a micropolar fluid past a sphere subjected to a constant surface temperature. In the analysis, the governing boundary layer equations are first transformed into a non-dimensional form, which contain

* Corresponding author.
E-mail address: popi@math.ubbcluj.ro (I. Pop).

1290-0729/02/$ – see front matter
doi:10.1016/S1290-0729(02)00027-3

Nomenclature

a	radius of the sphere ..... m
C_f	local skin friction coefficient
f	reduced stream function
g	acceleration due to gravity ..... $m{\cdot}s^{-2}$
Gr	Grashof number
h	reduced angular velocity of micropolar fluid
H	non-dimensional angular velocity of micropolar fluid
j	microinertia per unit mass ..... m^2
k	thermal conductivity ..... $W{\cdot}m^{-1}{\cdot}K^{-1}$
K	material parameter
Pr	Prandtl number
$Q_w(x)$	local heat transfer coefficient
$r(x)$	radial distance from symmetrical axis to surface of the sphere ..... m
Re	Reynolds number
T	fluid temperature ..... K
u, v	non-dimensional velocity components along x and y directions, respectively
$u_e(x)$	non-dimensional velocity outside boundary layer
U_∞	free stream velocity ..... $m{\cdot}s^{-1}$
x, y	non-dimensional Cartesian coordinates along the surface of the sphere and normal to it, respectively

Greek symbols

β	thermal expansion coefficient ..... K^{-1}
γ	spin gradient viscosity ..... $kg{\cdot}m{\cdot}s^{-1}$
κ	vortex viscosity ..... $kg{\cdot}m^{-1}{\cdot}s^{-1}$
λ	mixed convection parameter
μ	dynamic viscosity ..... $kg{\cdot}m^{-1}{\cdot}s^{-1}$
ν	kinematic viscosity ..... $m^2{\cdot}s^{-1}$
θ	non-dimensional temperature
ρ	density ..... $kg{\cdot}m^{-3}$
ψ	non-dimensional stream function

Superscripts

$'$	differentiation with respect to y
$\bar{}$	dimensional variables

Subscripts

w	condition at the wall
∞	ambient condition

only the material parameter K and the mixed convection parameter λ, with $\lambda > 0$ ($T_w > T_\infty$) for a heated sphere and $\lambda < 0$ ($T_w < T_\infty$) for a cooled sphere, respectively. For small values of $|\lambda|$ forced convection effects dominate, while for large values of $|\lambda|$ it is the natural convection, which is important, so that values of $|\lambda|$of O(1), where both effects are comparable, are of most interest. These equations are then solved numerically using the Keller-box method [18]. The effects of the material and mixed convection parameters on the local skin friction and local heat transfer coefficients as well as on the variation of the boundary layer separation point are illustrated through tables and graphs. The results are presented for the Prandtl number $Pr = 0.7$ and 7 (liquid water with polymeric molecules), respectively. Hence this paper is an extension of the previous work on this problem. It is shown that for a heated sphere ($\lambda > 0$) the separation of the boundary layer is delayed for each value of K considered, and it is found that there is a value of $\lambda = \lambda_K$ for which the boundary layer does not separate at all. On the other hand, the buoyancy forces retard the fluid and therefore the position of the boundary layer separation is brought nearer to the lower stagnation point of the sphere. A unique value of $\lambda = \lambda_K$ is found for each given value of K for which the boundary layer separates at this point. For values of λ less than λ_K a boundary layer solution is not possible.

Finally, it is worth mentioning that the present results for $K = 0$ (Newtonian fluid) are in agreement with those obtained recently by Nazar et al. [19].

2. Basic equations

Consider the steady mixed convection boundary layer flow about an impermeable sphere of radius a which is placed in a micropolar fluid flow with the undisturbed free stream velocity U_∞, and the constant temperature T_∞. The convective forced flow is assumed to be moving upward, while the gravity vector $\boldsymbol{g}$ acts downward in the opposite direction as shown in Fig. 1, where the coordinates $\bar{x}$ and $\bar{y}$ are chosen such that $\bar{x}$ measures the distance along the surface of the sphere from the lower stagnation point and $\bar{y}$ measures the distance normal to the surface of the sphere, respectively. It is assumed that the surface of the sphere is maintained at a constant temperature T_w with

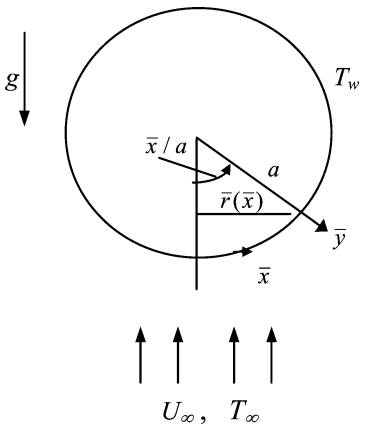

Fig. 1. Physical model and coordinate system.

$T_w > T_\infty$ corresponding to a heated sphere (aiding flow) or $T_w < T_\infty$ corresponding to a cooled sphere (opposing flow), respectively.

If $\bar{u}$ and $\bar{v}$ are the velocity components along $\bar{x}$ and $\bar{y}$ axes, $\overline{H}$ is the microrotation component normal to the $\bar{x}-\bar{y}$ plane and T is the fluid temperature, the equations which govern the boundary layer flow are

$$\frac{\partial}{\partial \bar{x}}(\bar{r}\bar{u}) + \frac{\partial}{\partial \bar{y}}(\bar{r}\bar{v}) = 0 \tag{1}$$

$$\bar{u}\frac{\partial \bar{u}}{\partial \bar{x}} + \bar{v}\frac{\partial \bar{u}}{\partial \bar{y}} = \bar{u}_e\frac{d\bar{u}_e}{d\bar{x}} + \left(\frac{\mu+\kappa}{\rho}\right)\frac{\partial^2 \bar{u}}{\partial \bar{y}^2} + g\beta(T-T_\infty)\sin\left(\frac{\bar{x}}{a}\right) + \frac{\kappa}{\rho}\frac{\partial \overline{H}}{\partial \bar{y}} \tag{2}$$

$$\rho j\left(\bar{u}\frac{\partial \overline{H}}{\partial \bar{x}} + \bar{v}\frac{\partial \overline{H}}{\partial \bar{y}}\right) = -\kappa\left(2\overline{H} + \frac{\partial \bar{u}}{\partial \bar{y}}\right) + \gamma\frac{\partial^2 \overline{H}}{\partial \bar{y}^2} \tag{3}$$

$$\bar{u}\frac{\partial T}{\partial \bar{x}} + \bar{v}\frac{\partial T}{\partial \bar{y}} = \frac{\nu}{Pr}\frac{\partial^2 T}{\partial \bar{y}^2} \tag{4}$$

subject to the boundary conditions:

$$\bar{u} = \bar{v} = 0, \quad T = T_w, \quad \overline{H} = -\frac{1}{2}\frac{\partial \bar{u}}{\partial \bar{y}} \quad \text{on } \bar{y} = 0 \tag{5a}$$

$$\bar{u} \to \bar{u}_e(\bar{x}), \quad \overline{H} \to 0, \quad T \to T_\infty \quad \text{as } \bar{y} \to \infty \tag{5b}$$

Here g is the magnitude of the acceleration due to gravity, β is the thermal expansion coefficient, ν is the kinematic viscosity, Pr is the Prandtl number, $\bar{r}(\bar{x})$ is the radial distance from the symmetrical axis to the surface of the sphere and $\bar{u}_e(\bar{x})$ is the local free stream velocity. These are given by

$$\bar{r}(\bar{x}) = a\sin(\bar{x}/a), \qquad \bar{u}_e(\bar{x}) = \frac{3}{2}U_\infty \sin(\bar{x}/a) \tag{6}$$

and we assume that $\gamma = (\mu + (\kappa/2))j$.

The following non-dimensional variables are now introduced

$$\begin{aligned} &x = \bar{x}/a, \qquad y = Re^{1/2}(\bar{y}/a) \\ &r(x) = \bar{r}(\bar{x})/a, \qquad u = \bar{u}/U_\infty \\ &v = Re^{1/2}(\bar{v}/U_\infty), \qquad u_e(x) = \bar{u}_e(\bar{x})/U_\infty \\ &H = (a/U_\infty)Re^{-1/2}\overline{H}, \qquad \theta = \frac{T-T_\infty}{T_w - T_\infty} \end{aligned} \tag{7}$$

where $Re = U_\infty a/\nu$ is the Reynolds number.

Using (7), the system of Eqs. (1)–(4) take the form

$$\frac{\partial}{\partial x}(ru) + \frac{\partial}{\partial y}(rv) = 0 \tag{8}$$

$$u\frac{\partial u}{\partial x} + v\frac{\partial u}{\partial y} = u_e\frac{du_e}{dx} + (1+K)\frac{\partial^2 u}{\partial y^2} + K\frac{\partial H}{\partial y} + \lambda\theta\sin x \tag{9}$$

$$u\frac{\partial H}{\partial x} + v\frac{\partial H}{\partial y} = -K\left(2H + \frac{\partial u}{\partial y}\right) + \left(1+\frac{K}{2}\right)\frac{\partial^2 H}{\partial y^2} \tag{10}$$

$$u\frac{\partial \theta}{\partial x} + v\frac{\partial \theta}{\partial y} = \frac{1}{Pr}\frac{\partial^2 \theta}{\partial y^2} \tag{11}$$

and the boundary conditions (5) become

$$u = v = 0, \quad \theta = 1, \quad H = -\frac{1}{2}\frac{\partial u}{\partial y} \quad \text{on } y = 0 \tag{12a}$$

$$u_e(x) \to \frac{3}{2}\sin x, \quad H \to 0, \quad \theta \to 0 \quad \text{as } y \to \infty \tag{12b}$$

where λ is the mixed convection parameter and K is the material parameter which are defined by

$$\lambda = \frac{Gr}{Re^2}, \qquad K = \frac{\kappa}{\mu} \tag{13}$$

with $Gr = g\beta(T_w - T_\infty)a^3/\nu^2$ being the Grashof number. It is worth mentioning that $\lambda > 0$ is for assisting flow (heated sphere) and $\lambda < 0$ for opposing flow (cooled sphere), respectively.

3. Solution

Eqs. (8)–(11) subject to the boundary condition (12) can be solved numerically using the Keller-box method described in the book by Cebeci and Bradshaw [18]. This method has been also very recently used by Nazar et al. [13–15] for solving some non-similar convective flow problems of Newtonian and micropolar fluids. Thus, since $\sin x/x \to 1$ as $x \to 0$, it is appropriate to introduce the transformation

$$\begin{aligned} &\psi = xr(x)f(x,y), \qquad \theta = \theta(x,y) \\ &H = xh(x,y) \end{aligned} \tag{14}$$

where ψ is the stream function defined in the usual way as

$$u = \frac{1}{r}\frac{\partial \psi}{\partial y}, \qquad v = -\frac{1}{r}\frac{\partial \psi}{\partial x} \tag{15}$$

Substituting (14) into Eqs. (9)–(11) we get, after some algebra, the following transformed equations

$$(1+K)\frac{\partial^3 f}{\partial y^3} + \left(1 + \frac{x}{\sin x}\cos x\right)f\frac{\partial^2 f}{\partial y^2} - \left(\frac{\partial f}{\partial y}\right)^2 + \frac{9}{4}\frac{\sin x\cos x}{x} + K\frac{\partial h}{\partial y} + \lambda\frac{\sin x}{x}\theta = x\left(\frac{\partial f}{\partial y}\frac{\partial^2 f}{\partial x\,\partial y} - \frac{\partial f}{\partial x}\frac{\partial^2 f}{\partial y^2}\right) \tag{16}$$

$$\left(1+\frac{K}{2}\right)\frac{\partial^2 h}{\partial y^2} + \left(1 + \frac{x}{\sin x}\cos x\right)f\frac{\partial h}{\partial y} - \frac{\partial f}{\partial y}h - K\left(2h + \frac{\partial^2 f}{\partial y^2}\right) = x\left(\frac{\partial f}{\partial y}\frac{\partial h}{\partial x} - \frac{\partial f}{\partial x}\frac{\partial h}{\partial y}\right) \tag{17}$$

$$\frac{1}{Pr}\frac{\partial^2 \theta}{\partial y^2} + \left(1 + \frac{x}{\sin x}\cos x\right)f\frac{\partial \theta}{\partial y} = x\left(\frac{\partial f}{\partial y}\frac{\partial \theta}{\partial x} - \frac{\partial f}{\partial x}\frac{\partial \theta}{\partial y}\right) \tag{18}$$

and the boundary conditions (12) become

$$f=0,\quad \frac{\partial f}{\partial y}=0,\quad \theta=1,\quad h=-\frac{1}{2}\frac{\partial^2 f}{\partial y^2}\quad \text{on } y=0 \tag{19a}$$

$$\frac{\partial f}{\partial y}\to\frac{3}{2}\frac{\sin x}{x},\quad h\to 0,\quad \theta\to 0\quad \text{as } y\to\infty \tag{19b}$$

We notice that at the lower stagnation point of the sphere, $x\approx 0$, Eqs. (16)–(18) reduce to

$$(1+K)f'''+2ff''-f'^2+Kh'+\lambda\theta+\frac{9}{4}=0 \tag{20}$$

$$\left(1+\frac{K}{2}\right)h''+2fh'-f'h-K\left(2h+f''\right)=0 \tag{21}$$

$$\frac{1}{Pr}\theta''+2f\theta'=0 \tag{22}$$

subject to the boundary conditions

$$\begin{aligned} &f(0)=f'(0)=0,\qquad \theta(0)=1\\ &h(0)=-\frac{1}{2}f''(0)\end{aligned} \tag{23a}$$

$$f'\to\frac{3}{2},\quad h\to 0,\quad \theta\to 0\quad \text{as } y\to\infty \tag{23b}$$

where primes denote differentiation with respect to y.

The physical quantities of primary interest are the local skin friction coefficient, C_f, and the local wall heat transfer coefficient , Q_w, which are defined as

$$\begin{aligned} C_f&=\frac{a}{U_\infty}Re^{-1/2}\left[(\mu+\kappa)\frac{\partial\bar{u}}{\partial\bar{y}}+\kappa\overline{H}\right]_{\bar{y}=0}\\ Q_w&=-\frac{a}{k(T_w-T_\infty)}Re^{-1/2}\left(\frac{\partial T}{\partial\bar{y}}\right)_{\bar{y}=0}\end{aligned} \tag{24}$$

Using the non-dimensional variables (7), we have

$$C_f=x\left(1+\frac{K}{2}\right)\left(\frac{\partial^2 F}{\partial y^2}\right)_{y=0},\qquad Q_w(x)=-\left(\frac{\partial\theta}{\partial y}\right)_{y=0} \tag{25}$$

We notice that for $\lambda>0$, an asymptotic solution of Eqs. (20)–(22) for large values of λ ($\gg 1$) can be determined if we make the transformation

$$\begin{aligned} &f(y)=\lambda^{1/4}F(\eta),\qquad h=\lambda^{3/4}H(y)\\ &\theta(y)=G(\eta),\qquad \eta=\lambda^{1/4}y\end{aligned} \tag{26}$$

Substituting (26) into Eqs. (20)–(22) these reduce to

$$(1+K)F'''+2FF''-F'^2+KH'+G+\frac{9}{4}\lambda^{-1}=0 \tag{27}$$

$$\left(1+\frac{K}{2}\right)H''+2FH'-F'H-K\lambda^{-1/2}\left(2H+F''\right)=0 \tag{28}$$

$$\frac{1}{Pr}G''+2FG'=0 \tag{29}$$

subject to the boundary conditions

$$\begin{aligned} &F(0)=F'(0)=0,\qquad G(0)=1\\ &H(0)=-\frac{1}{2}F''(0)\end{aligned} \tag{30a}$$

$$F'\to\frac{3}{2}\lambda^{-1/2},\quad H\to 0,\quad G\to 0\quad \text{as } \eta\to\infty \tag{30b}$$

where primes now denote differentiation with respect to η.

A solution of Eqs. (27)–(29) is sought in the form of series

$$\begin{aligned} F&=F_0(\eta)+\lambda^{-1/2}F_1(\eta)+\lambda^{-1}F_2(\eta)+\cdots\\ G&=G_0(\eta)+\lambda^{-1/2}G_1(\eta)+\lambda^{-1}G_2(\eta)+\cdots\\ H&=H_0(\eta)+\lambda^{-1/2}H_1(\eta)+\lambda^{-1}H_2(\eta)+\cdots\end{aligned} \tag{31}$$

where F_0, H_0 and G_0 are given by

$$(1+K)F_0'''+2F_0F_0''-F_0'^2+KH_0'+G_0=0 \tag{32}$$

$$\left(1+\frac{K}{2}\right)H_0''+2F_0H_0'-F_0'H_0=0 \tag{33}$$

$$\frac{1}{Pr}G_0''+2F_0G_0'=0 \tag{34}$$

subject to the boundary conditions

$$\begin{aligned} &F_0(0)=F_0'(0)=0,\qquad G_0(0)=1\\ &H_0(0)=-\frac{1}{2}F_0''(0)\end{aligned} \tag{35a}$$

$$F_0'\to 0,\quad G_0\to 0,\quad H_0\to 0\quad \text{as } \eta\to\infty \tag{35b}$$

These equations describe the free convection from the lower stagnation point of an isothermal sphere, see Nazar et al. [15], while the equations for the functions $F_i(\eta)$, $H_i(\eta)$ and $G_i(\eta)$, $i\geqslant 1$ can be written as

$$\begin{aligned}&(1+K)F_i'''+2\sum_{j=0}^{i}F_{i-j}F_j''\\ &\quad-\sum_{j=0}^{i}F_{i-j}'F_j'+KH_i'+G_i+\frac{9}{4}\delta_{2i}=0\end{aligned} \tag{36}$$

$$\begin{aligned}&\left(1+\frac{K}{2}\right)H_i''+2\sum_{j=0}^{i}F_{i-j}H_j'\\ &\quad-\sum_{j=0}^{i}F_{i-j}'H_j-K\left(2H_i+F_i''\right)=0\end{aligned} \tag{37}$$

$$\frac{1}{Pr}G_i''+2\sum_{j=0}^{i}F_{i-j}G_j'=0 \tag{38}$$

along with the boundary conditions

$$\begin{aligned} &F_i(0)=F_i'(0)=0,\qquad G_i'(0)=0\\ &H_i(0)=-\frac{1}{2}F_i''(0)\end{aligned} \tag{39a}$$

$$F_i'\to\frac{3}{2}\delta_{1i},\quad G_i\to 0,\quad H_i\to 0\quad \text{as } \eta\to\infty \tag{39b}$$

where δ_{1i} and δ_{2i} are the Kronecker delta operators. Thus, we have

$$f''(0) = \lambda^{3/4}\left[F_0''(0) + \lambda^{-1/2}F_1''(0) + \lambda^{-1}F_2''(0) + \cdots\right] \tag{40a}$$

$$-\theta'(0) = \lambda^{1/4}\left[G_0'(0) + \lambda^{-1/2}G_1'(0) + \lambda^{-1}G_2'(0) + \cdots\right] \tag{40b}$$

for $\lambda \gg 1$.

4. Results and discussion

Solutions of the system of the non-similar boundary layer Eqs. (16)–(18) subject to the boundary conditions (19) were obtained numerically using the Keller-box method along with the Newton's linearization technique as described by Cebeci and Bradshaw [18]. The numerical solution starts at the lower stagnation point of the sphere, $x \approx 0$, with the initial profiles as given by Eqs. (20)–(22) and proceed round the sphere up to the separation point. Representative results for the local skin friction coefficient C_f and the local heat transfer coefficient $Q_w(x)$ have been obtained at different positions $0° \leqslant x \leqslant 120°$ for $K = 0$, 0.5, 1, 1.5, 2, 2.5 and 3 and various values of the mixed convection parameter λ when $Pr = 0.7$ and $Pr = 7$ (liquid water with polymeric molecules), respectively. It should be noticed that the present results were obtained up to the value of $x = 120°$, while those of Lien and Chen [16] terminate at $x = 90°$. However, in order to save space, we will give here results only for $K = 0$ and 1.

The values of $f''(0)$ and $-\theta'(0)$ obtained by numerically solving Eqs. (20)–(22) subject to the boundary conditions (23) for some values of λ and $K = 0$ and 1 are presented in Table 1 for $Pr = 0.7$ and in Table 2 for $Pr = 7$. The values obtained from the asymptotic series (40) for $\lambda > 0$ and large values of λ ($\gg 1$) are also included in these tables and these show good agreement with the numerical results even at moderate values of λ. We notice that the value of $-G_0'(0) = 0.4576$ for $K = 0$ and $Pr = 0.7$, obtained by solving Eqs. (32)–(34) subject to the boundary conditions (35), is in very good agreement with that obtained by Chiang et al. [20], which is 0.4576. We also mention that the present results for $K = 0$, $Pr = 0.7$ and various values of λ are in complete agreement with those reported recently by Nazar et al. [19]. We are therefore confident that the results presented in this paper are very accurate.

Further, Tables 3–10 show the values of C_f and $Q_w(x)$ for $K = 0$ and 1 at different positions x and different values of λ for $Pr = 0.7$ and 7, respectively. The variation of C_f and $Q_w(x)$ is also illustrated in Figs. 2–9. It can be seen from these tables and figures that the values of C_f are lower while the values of $Q_w(x)$ are higher for $K = 0$ (Newtonian fluid) than for $K = 1$. It can also be seen that the values of C_f are lower, while those of $Q_w(x)$are higher for $Pr = 7$ than for $Pr = 0.7$ when the parameters K, x and λ are fixed. It is also seen from these tables and figures that for the aiding flow C_f and $Q_w(x)$ increase as the mixed convection or the buoyancy force increases, while an opposite trend is observed for opposing flow. Also, for given values of K and λ, the heat transfer coefficient is seen to decrease with the increasing distance x from the stagnation point. Further, we can see from these tables and figures, as expected, the boundary layer separates from the sphere for some negative values of λ (opposing flow) and also for some positive values of λ (assisting flow). Opposing flow brings the separation point close to the lower stagnation point and for sufficiently large negative values of λ or sufficiently strong opposing flow, there will not be a boundary layer on the sphere. Increasing λ delays the

Table 1
Values of $f''(0)$ and $-\theta'(0)$ for various values of λ, $K = 0$ and 1 for $Pr = 0.7$

λ	Numerical ($K = 0$)		Series ($K = 0$)		λ	Numerical ($K = 1$)		Series ($K = 1$)	
	$f''(0)$	$-\theta'(0)$	$f''(0)$	$-\theta'(0)$		$f''(0)$	$-\theta'(0)$	$f''(0)$	$-\theta'(0)$
−4.7	−0.0081	0.5892			−5.8	−0.0318	0.5444		
−4.6	0.0770	0.6011			−5.7	0.0205	0.5534		
−4.5	0.1566	0.6117			−5.0	0.3295	0.6014		
−4.0	0.5028	0.6534			−4.0	0.6440	0.6418		
−3.0	1.0700	0.7108			−3.0	0.9383	0.6770		
−2.0	1.5581	0.7529			−2.0	1.2113	0.7064		
−1.0	2.0016	0.7870			−1.0	1.4617	0.7312		
−0.5	2.2115	0.8021			−0.5	1.5840	0.7427		
0.0	2.4151	0.8162			0.0	1.7042	0.7536		
1.0	2.8064	0.8463	2.9966	0.9344	1.0	1.9444	0.7745	2.0855	0.8472
2.0	3.1804	0.8648	3.2484	1.0008	2.0	2.1750	0.7935	2.2901	0.8468
3.0	3.5401	0.8857	3.5251	1.0615	3.0	2.3976	0.8109	2.5119	0.8711
4.0	3.8880	0.9050	3.7965	1.1138	4.0	2.6134	0.8271	2.7292	0.8976
5.0	4.2257	0.9230	4.0587	1.1594	5.0	2.8271	0.8425	2.9392	0.9232
6.0	4.5546	0.9397	4.3116	1.2000	6.0	3.0318	0.8568	3.1420	0.9472
7.0	4.8756	0.9555	4.5561	1.2367	7.0	3.2318	0.8702	3.3383	0.9696
8.0	5.1896	0.9704	4.7931	1.2702	8.0	3.4323	0.8833	3.5288	0.9906
9.0	5.4974	0.9846	5.0235	1.3011	9.0	3.6244	0.8954	3.7141	1.0103
10.0	5.7995	0.9981	5.2478	1.3298	10.0	3.8131	0.9070	3.8948	1.0289
20.0	8.5876	1.1077	7.2592	1.5451	20.0	5.5713	1.0029	5.5210	1.1732

Table 2
Values of $f''(0)$ and $-\theta'(0)$ for various values of λ, $K = 0$ and 1 for $Pr = 7$

λ	Numerical ($K = 0$)		Series ($K = 0$)		λ	Numerical ($K = 1$)		Series ($K = 1$)	
	$f''(0)$	$-\theta'(0)$	$f''(0)$	$-\theta'(0)$		$f''(0)$	$-\theta'(0)$	$f''(0)$	$-\theta'(0)$
−8.3	−0.0065	1.3920			−10.9	−0.0410	1.2630		
−8.2	0.0391	1.4057			−10.8	0.0263	1.2838		
−8.0	0.1266	1.4313			−10.0	0.2306	1.3566		
−7.0	0.4309	1.5006			−8.0	0.6459	1.4847		
−6.0	0.7887	1.5917			−6.0	0.8872	1.5399		
−5.0	1.1025	1.6631			−5.0	1.0549	1.5834		
−4.0	1.3947	1.7251			−4.0	1.2142	1.6226		
−3.0	1.6685	1.7795			−3.0	1.3319	1.6483		
−2.0	1.9280	1.8281			−2.0	1.4465	1.6726		
−1.0	2.1762	1.8723			−1.0	1.5687	1.6986		
0.0	2.4151	1.9130			0.0	1.7042	1.7275		
1.0	2.6462	1.9508	2.8049	2.0823	1.0	1.8400	1.7559	2.0305	1.9490
2.0	2.8702	1.9862	3.0454	2.0445	2.0	1.9725	1.7826	2.1307	1.8923
3.0	3.0887	2.0195	3.2935	2.0651	3.0	2.1018	1.8081	2.2591	1.8959
4.0	3.3017	2.0509	3.5310	2.0971	4.0	2.2285	1.8323	2.4085	1.9135
5.0	3.5101	2.0808	3.7572	2.1314	5.0	2.3526	1.8555	2.5442	1.9354
6.0	3.7142	2.1093	3.9734	2.1654	6.0	2.4783	1.8786	2.6854	1.9585
7.0	3.9145	2.1365	4.1810	2.1983	7.0	2.5980	1.8999	2.8020	1.9818
8.0	4.1112	2.1626	4.3810	2.2300	8.0	2.7205	1.9215	2.9445	2.0046
9.0	4.3047	2.1877	4.5744	2.2602	9.0	2.8425	1.9426	3.0930	2.0268
10.0	4.4952	2.2119	4.7622	2.2892	10.0	2.9568	1.9617	3.2381	2.0483
20.0	6.2720	2.4162	6.4234	2.5246	20.0	4.0618	2.1319	4.4480	2.2292

Table 3
Values of local skin friction coefficient C_f for $K = 0$, $Pr = 0.7$ and various values of λ

x	λ										
	−4.0	−3.0	−2.0	−1.0	−0.5	0.0	0.74	0.75	1.0	2.0	5.0
0°	0.0000	0.0000	0.0000	0.0000	0.0000	0.0000	0.0000	0.0000	0.0000	0.0000	0.0000
10°	0.0801	0.1806	0.2662	0.3438	0.3804	0.4160	0.4669	0.4675	0.4843	0.5495	0.7318
20°	0.1149	0.3261	0.5000	0.6564	0.7301	0.8014	0.9031	0.9045	0.9380	1.0682	1.4314
30°		0.4024	0.6718	0.9098	1.0211	1.1284	1.2813	1.2833	1.3335	1.5284	2.0700
40°		0.3704	0.7535	1.0790	1.2292	1.3733	1.5775	1.5802	1.6471	1.9061	2.6223
50°			0.7181	1.1434	1.3350	1.5172	1.7737	1.7771	1.8607	2.1832	3.0688
60°			0.5295	1.0866	1.3246	1.5477	1.8580	1.8621	1.9627	2.3481	3.3962
70°				0.8929	1.1889	1.4583	1.8260	1.8307	1.9486	2.3967	3.5988
80°				0.5280	0.9190	1.2480	1.6800	1.6855	1.8216	2.3326	3.6779
90°					0.4813	0.9154	1.4289	1.4352	1.5915	2.1668	3.6417
100°						0.4308	1.0847	1.0922	1.2732	1.9166	3.5038
110°							0.6543	0.6637	0.8831	1.6049	3.2819
120°								0.0380	0.4220	1.2579	2.9950

Table 4
Values of local heat transfer coefficient $Q_w(x)$ for $K = 0$, $Pr = 0.7$ and various values of λ

x	λ										
	−4.0	−3.0	−2.0	−1.0	−0.5	0.0	0.74	0.75	1.0	2.0	5.0
0°	0.6534	0.7108	0.7529	0.7870	0.8021	0.8162	0.8354	0.8357	0.8463	0.8648	0.9230
10°	0.6440	0.7040	0.7470	0.7818	0.7970	0.8112	0.8307	0.8309	0.8371	0.8603	0.9188
20°	0.6150	0.6845	0.7305	0.7669	0.7827	0.7974	0.8173	0.8176	0.8239	0.8476	0.9070
30°		0.6507	0.7027	0.7422	0.7591	0.7746	0.7955	0.7958	0.8024	0.8269	0.8878
40°		0.5977	0.6628	0.7076	0.7261	0.7429	0.7652	0.7655	0.7725	0.7983	0.8614
50°			0.6080	0.6624	0.6836	0.7022	0.7267	0.7270	0.7345	0.7621	0.8281
60°			0.5309	0.6055	0.6309	0.6525	0.6800	0.6803	0.6887	0.7186	0.7884
70°				0.5334	0.5668	0.5934	0.6253	0.6257	0.6352	0.6683	0.7426
80°				0.4342	0.4879	0.5236	0.5627	0.5632	0.5742	0.6117	0.6914
90°					0.3796	0.4398	0.4920	0.4926	0.5060	0.5495	0.6356
100°						0.3263	0.4120	0.4127	0.4304	0.4826	0.5758
110°							0.3179	0.3192	0.3458	0.4121	0.5130
120°								0.1276	0.2442	0.3391	0.4477

Table 5
Values of local skin friction coefficient C_f for $K = 0$, $Pr = 7$ and various values of λ

x	λ										
	−7.0	−5.0	−3.0	−2.0	−1.0	0.0	1.07	1.08	2.0	5.0	10.0
0°	0.0000	0.0000	0.0000	0.0000	0.0000	0.0000	0.0000	0.0000	0.0000	0.0000	0.0000
10°	0.0676	0.1872	0.2856	0.3309	0.3743	0.4160	0.4591	0.4595	0.4955	0.6071	0.7788
20°		0.3415	0.5396	0.6304	0.7176	0.8014	0.8877	0.8885	0.9605	1.1833	1.5256
30°		0.4311	0.7329	0.8700	1.0020	1.1284	1.2584	1.2595	1.3675	1.7009	2.2115
40°			0.8389	1.0242	1.2030	1.3733	1.5474	1.5490	1.6931	2.1361	2.8115
50°			0.8325	1.0713	1.3008	1.5172	1.7367	1.7387	1.9194	2.4707	3.3058
60°				0.9922	1.2808	1.5477	1.8147	1.8171	2.0350	2.6933	3.6815
70°				0.7635	1.1323	1.4583	1.7769	1.7798	2.0363	2.8002	3.9326
80°					0.8416	1.2480	1.6263	1.6296	1.9273	2.7952	4.0603
90°					0.3429	0.9154	1.3719	1.3759	1.7195	2.6900	4.0726
100°						0.4308	1.0272	1.0319	1.4313	2.5026	3.9829
110°							0.6018	0.6079	1.0870	2.2559	3.8079
120°								0.0153	0.7152	1.9757	3.5654

Table 6
Values of local heat transfer coefficient $Q_w(x)$ for $K = 0$, $Pr = 7$ and various values of λ

x	λ										
	−7.0	−5.0	−3.0	−2.0	−1.0	0.0	1.07	1.08	2.0	5.0	10.0
0°	1.5006	1.6645	1.7795	1.8281	1.8723	1.9130	1.9534	1.9568	1.9862	2.0808	2.2119
10°	1.4779	1.6489	1.7656	1.8148	1.8596	1.9008	1.9415	1.9418	1.9746	2.0699	2.2017
20°		1.6043	1.7263	1.7771	1.8236	1.8662	1.9082	1.9086	1.9420	2.0394	2.1731
30°		1.5281	1.6608	1.7147	1.7644	1.8095	1.8536	1.8540	1.8890	1.9895	2.1266
40°			1.5672	1.6267	1.6815	1.7307	1.7780	1.7784	1.8156	1.9210	2.0627
50°			1.4411	1.5110	1.5744	1.6297	1.6818	1.6823	1.7226	1.8348	1.9824
60°				1.3629	1.4412	1.5062	1.5654	1.5659	1.6108	1.7320	1.8871
70°				1.1683	1.2775	1.3590	1.4291	1.4297	1.4809	1.6140	1.7780
80°					1.0702	1.1848	1.2726	1.2733	1.3338	1.4828	1.6569
90°					0.7502	0.9735	1.0947	1.0956	1.1707	1.3406	1.5258
100°						0.6791	0.8913	0.8926	0.9923	1.1901	1.3866
110°							0.6462	0.6485	0.7992	1.0349	1.2414
120°								0.1590	0.5907	0.8788	1.0921

Table 7
Values of local skin friction coefficient C_f for $K = 1$, $Pr = 0.7$ and various values of λ

x	λ										
	−5.0	−4.0	−3.0	−2.0	−1.0	0.0	0.76	0.77	1.0	2.0	5.0
0°	0.0000	0.0000	0.0000	0.0000	0.0000	0.0000	0.0000	0.0000	0.0000	0.0000	0.0000
10°	0.0629	0.1618	0.2394	0.3112	0.3768	0.4403	0.4884	0.4890	0.5032	0.5636	0.7341
20°	0.0727	0.2852	0.4439	0.5890	0.7210	0.8484	0.9446	0.9458	0.9742	1.0948	1.4348
30°		0.3308	0.5804	0.8029	1.0030	1.1949	1.3394	1.3413	1.3840	1.5645	2.0720
40°		0.2441	0.6160	0.9252	1.1969	1.4549	1.6482	1.6507	1.7075	1.9578	2.6196
50°			0.5112	0.9307	1.2815	1.6087	1.8516	1.8547	1.9259	2.2255	3.0576
60°				0.7932	1.2409	1.6432	1.9375	1.9412	2.0270	2.3859	3.3727
70°					1.0617	1.5523	1.9013	1.9058	2.0065	2.4249	3.5596
80°					0.7221	1.3357	1.7464	1.7515	1.8682	2.3470	3.6209
90°						0.9942	1.4826	1.4886	1.6230	2.1644	3.5665
100°						0.5063	1.1244	1.1314	1.2878	1.8968	3.4122
110°							0.6818	0.6906	0.8813	1.5695	3.1786
120°								0.0436	0.4062	1.2125	2.8872

separation and that separation can be completely suppressed in the region $0° \leqslant x \leqslant 120°$ for sufficiently large values of λ (> 0). Moreover, the numerical solutions indicate that for $K = 0$ the value of λ, which first gives no separation lies between 0.74 and 0.75 for $Pr = 0.7$, while the value of λ (> 0) lies between 1.07 and 1.08 for $Pr = 7$. When $K = 1$, the value of λ (> 0) lies between 0.76 and 0.77 for $Pr = 0.7$, while it lies between 1.09 and 1.10 for $Pr = 7$. This value of λ increases as the material parameter K increases.

Table 8
Values of local heat transfer coefficient $Q_w(x)$ for $K = 1$, $Pr = 0.7$ and various values of λ

x	λ										
	−5.0	−4.0	−3.0	−2.0	−1.0	0.0	0.76	0.77	1.0	2.0	5.0
0°	0.5905	0.6418	0.6770	0.7064	0.7312	0.7536	0.7697	0.7699	0.7745	0.7935	0.8425
10°	0.5810	0.6352	0.6713	0.7013	0.7264	0.7491	0.7653	0.7655	0.7701	0.7893	0.8386
20°	0.5504	0.6159	0.6550	0.6867	0.7128	0.7362	0.7529	0.7531	0.7579	0.7774	0.8276
30°		0.5816	0.6274	0.6623	0.6904	0.7151	0.7326	0.7328	0.7378	0.7581	0.8097
40°		0.5233	0.5866	0.6277	0.6589	0.6858	0.7045	0.7047	0.7100	0.7314	0.7849
50°			0.5269	0.5813	0.6180	0.6481	0.6686	0.6689	0.6746	0.6975	0.7538
60°				0.5195	0.5667	0.6021	0.6252	0.6254	0.6318	0.6569	0.7166
70°					0.5029	0.5473	0.5742	0.5746	0.5818	0.6098	0.6738
80°					0.4191	0.4826	0.5158	0.5162	0.5248	0.5568	0.6261
90°						0.4052	0.4497	0.4501	0.4607	0.4984	0.5741
100°						0.3020	0.3746	0.3752	0.3893	0.4355	0.5187
110°							0.2857	0.2868	0.3087	0.3691	0.4607
120°								0.1163	0.2091	0.3004	0.4011

Table 9
Values of local skin friction coefficient C_f for $K = 1$, $Pr = 7$ and various values of λ

x	λ											
	−10.0	−8.0	−6.0	−4.0	−2.0	−1.0	0.0	1.09	1.10	2	5	10
0°	0.0000	0.0000	0.0000	0.0000	0.0000	0.0000	0.0000	0.0000	0.0000	0.0000	0.0000	0.0000
10°	0.0532	0.1635	0.2261	0.3025	0.3728	0.4048	0.4403	0.4791	0.4794	0.5106	0.6111	0.7681
20°		0.2954	0.4178	0.5718	0.7130	0.7772	0.8484	0.9260	0.9267	0.9891	1.1898	1.5029
30°			0.5422	0.7772	0.9909	1.0876	1.1949	1.3117	1.3128	1.4064	1.7072	2.1745
40°				0.8905	1.1804	1.3104	1.4549	1.6115	1.6129	1.7380	2.1382	2.7569
50°				0.8849	1.2599	1.4254	1.6087	1.8061	1.8079	1.9650	2.4641	3.2301
60°					1.2122	1.4177	1.6432	1.8836	1.8858	2.0755	2.6733	3.5812
70°					1.0212	1.2779	1.5523	1.8395	1.8420	2.0660	2.7621	3.8050
80°						0.9966	1.3357	1.6771	1.6801	1.9410	2.7356	3.9043
90°						0.5382	0.9942	1.4068	1.4103	1.7132	2.6070	3.8893
100°							0.5063	1.0436	1.0478	1.4030	2.3971	3.7764
110°								0.5995	0.6050	1.0379	2.1327	3.5862
120°									0.0126	0.6531	1.8443	3.3403

Table 10
Values of local heat transfer coefficient $Q_w(x)$ for $K = 1$, $Pr = 7$ and various values of λ

x	λ											
	−10.0	−8.0	−6.0	−4.0	−2.0	−1.0	0.0	1.09	1.10	2	5	10
0°	1.3566	1.4847	1.5399	1.6118	1.6726	1.6986	1.7275	1.7583	1.7586	1.7826	1.8564	1.9617
10°	1.3385	1.4718	1.5265	1.5994	1.6610	1.6872	1.7165	1.7476	1.7479	1.7722	1.8465	1.9524
20°		1.4348	1.4879	1.5643	1.6283	1.6553	1.6856	1.7176	1.7179	1.7428	1.8188	1.9263
30°			1.4223	1.5057	1.5741	1.6027	1.6346	1.6683	1.6686	1.6947	1.7734	1.8839
40°				1.4220	1.4980	1.5292	1.5639	1.6001	1.6004	1.6281	1.7111	1.8255
50°				1.3092	1.3990	1.4343	1.4733	1.5132	1.5135	1.5437	1.6324	1.7522
60°					1.2742	1.3169	1.3624	1.4078	1.4082	1.4419	1.5385	1.6650
70°					1.1169	1.1737	1.2303	1.2842	1.2847	1.3234	1.4306	1.5653
80°						0.9961	1.0741	1.1419	1.1425	1.1888	1.3102	1.4547
90°						0.7481	0.8855	0.9796	0.9803	1.0386	1.1795	1.3352
100°							0.6288	0.7927	0.7938	0.8732	1.0412	1.2089
110°								0.5641	0.5660	0.6922	0.8986	1.0782
120°									0.0519	0.4930	0.7564	0.9454

Figs. 10–13 illustrate the variation of the separation point x_s with λ for $K = 0$ and 1 when $Pr = 0.7$ and 7, respectively. It is seen that for each value of K and Pr there is a value of λ (< 0) below which a boundary layer separation is not possible. The reason is that for $\lambda < 0$ the opposing flow is strong enough and the free convection boundary layer would start at the position x between 90° and 120° (see Chiang et al. [20]) and for sufficiently small values of $\lambda = \lambda_K$ (say), there comes a point where the flow of the free stream upwards cannot overcome the tendency of the fluid

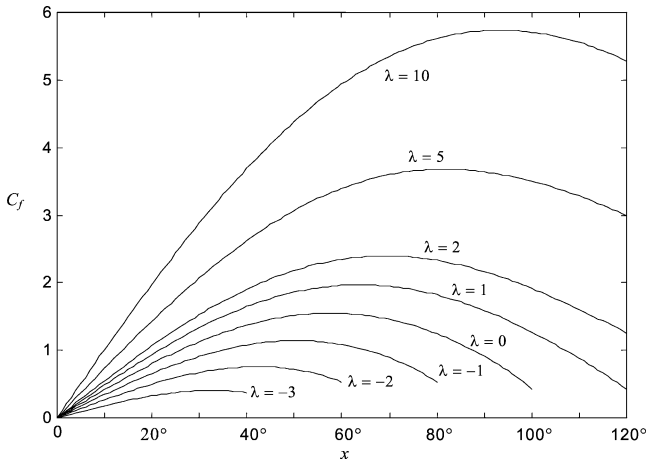

Fig. 2. Variation of the local skin friction coefficient C_f for $K = 0$, $Pr = 0.7$ and various values of λ.

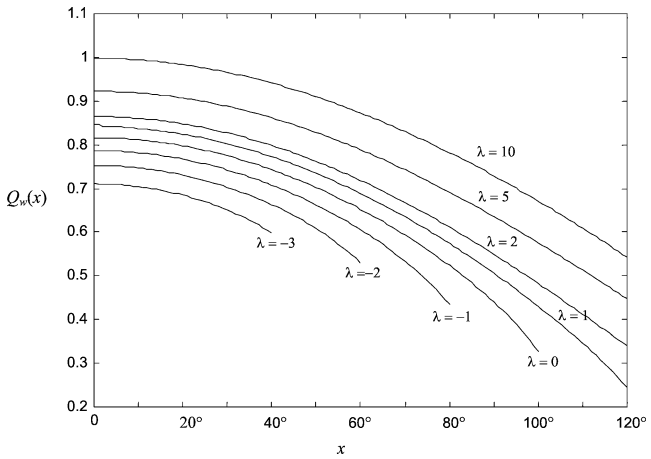

Fig. 3. Variation of the local heat transfer coefficient $Q_w(x)$ for $K = 0$, $Pr = 0.7$ and various values of λ.

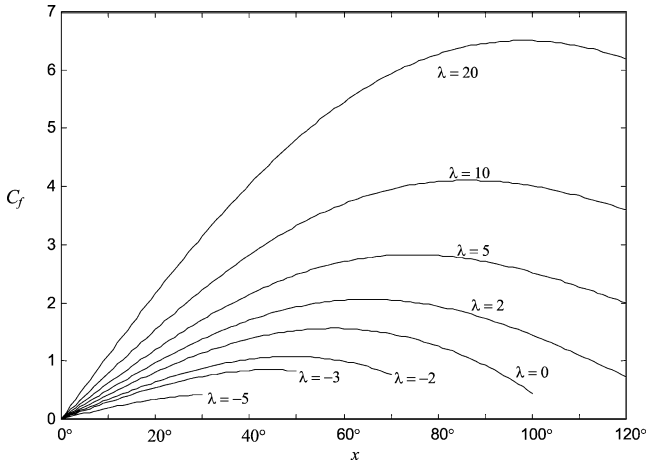

Fig. 4. Variation of the local skin friction coefficient C_f for $K = 0$, $Pr = 7$ and various values of λ.

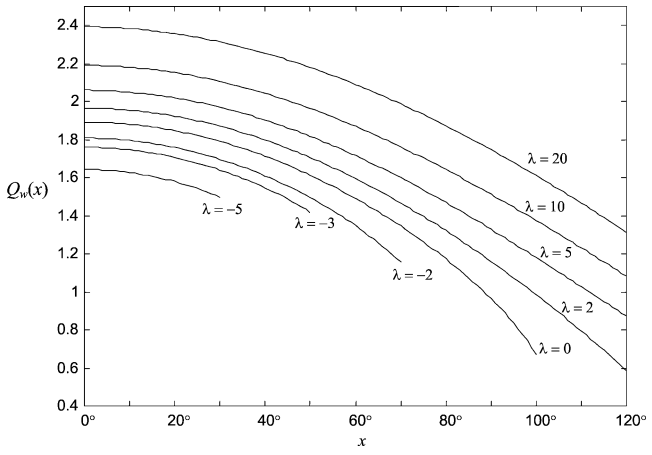

Fig. 5. Variation of the local heat transfer coefficient $Q_w(x)$ for $K = 0$, $Pr = 7$ and various values λ.

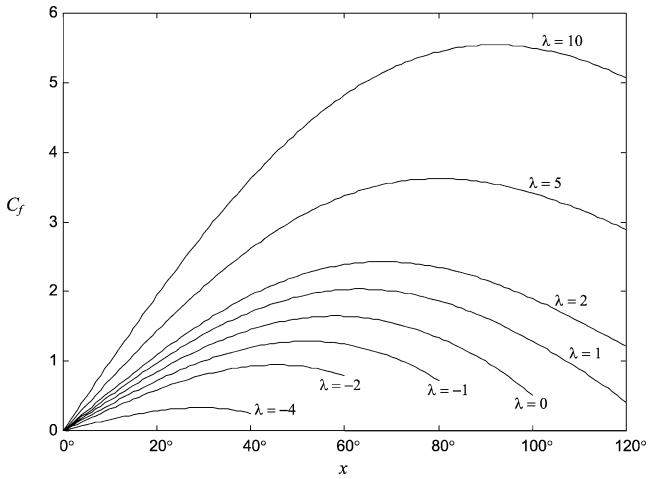

Fig. 6. Variation of the local skin friction coefficient C_f for $K = 1$, $Pr = 0.7$ and various values of λ.

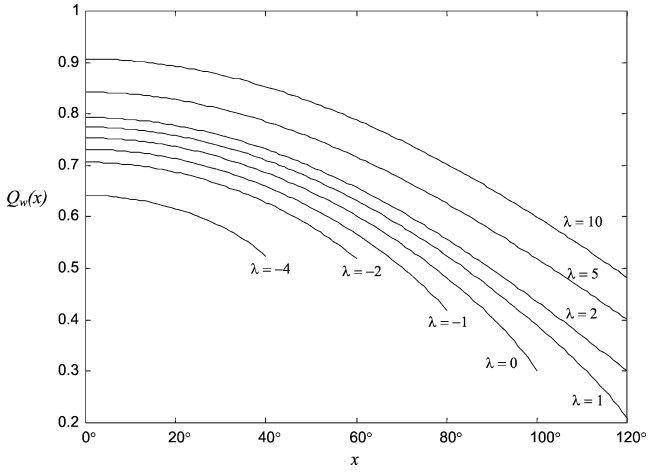

Fig. 7. Variation of the local heat transfer coefficient $Q_w(x)$ for $K = 1$, $Pr = 0.7$ and various values of λ.

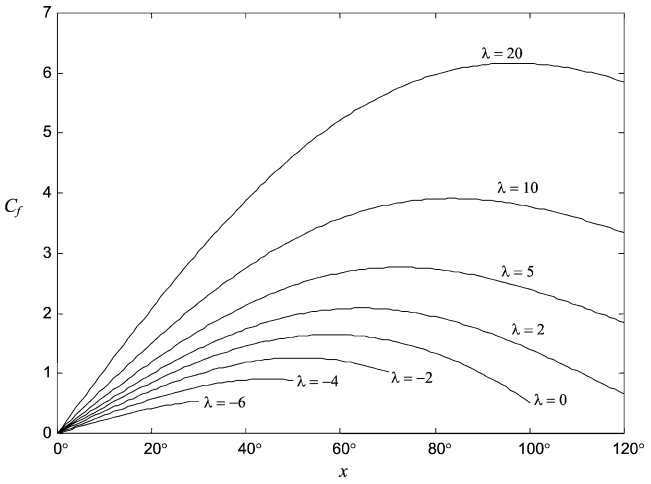

Fig. 8. Variation of the local skin friction coefficient C_f for $K = 1$, $Pr = 7$ and various values of λ

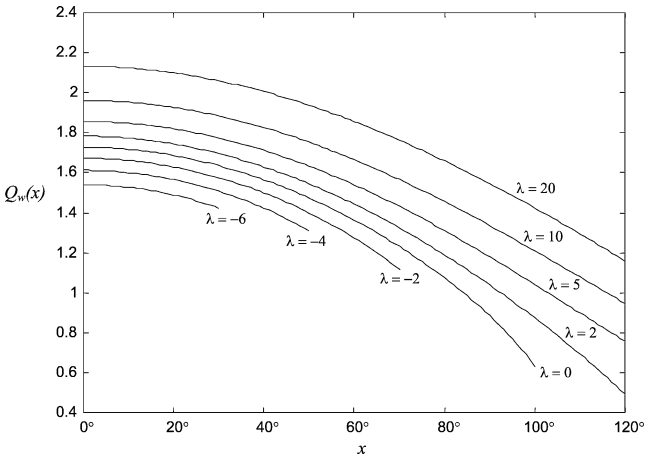

Fig. 9. Variation of the local heat transfer coefficient $Q_w(x)$ for $K = 1$, $Pr = 7$ and various values of λ.

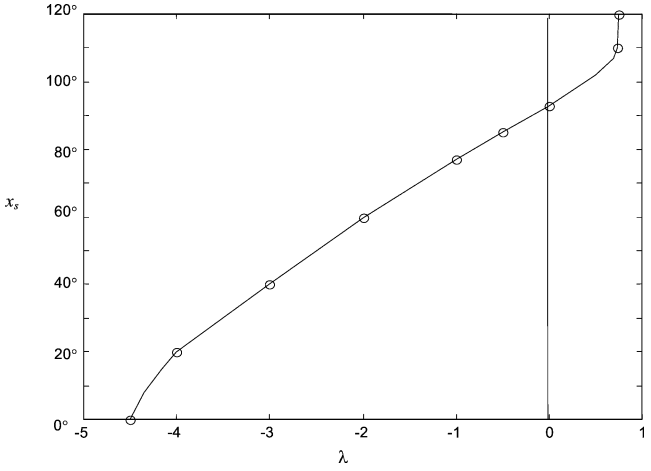

Fig. 10. Variation of the boundary layer separation point x_s with λ for $K = 0$ and $Pr = 0.7$.

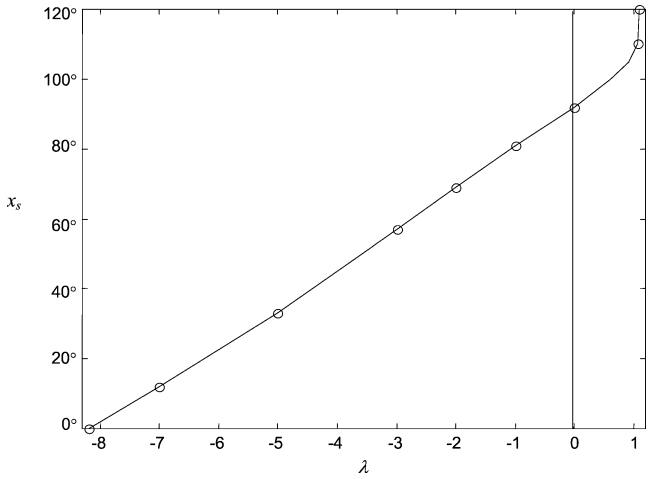

Fig. 11. Variation of the boundary layer separation point x_s with λ for $K = 0$ and $Pr = 7$.

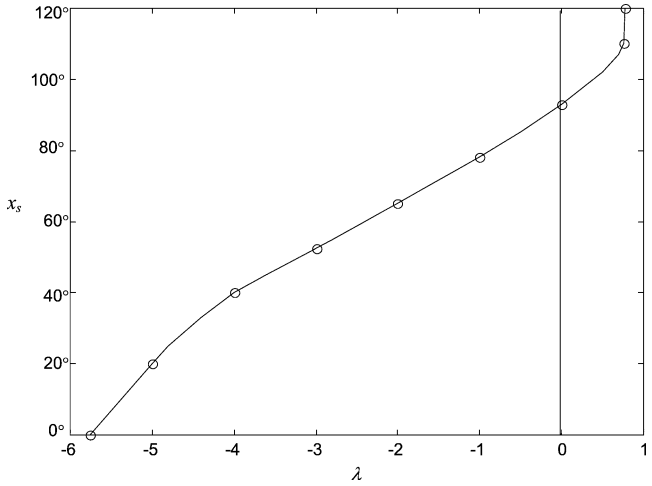

Fig. 12. Variation of the boundary layer separation point x_s with λ for $K = 1$ and $Pr = 0.7$.

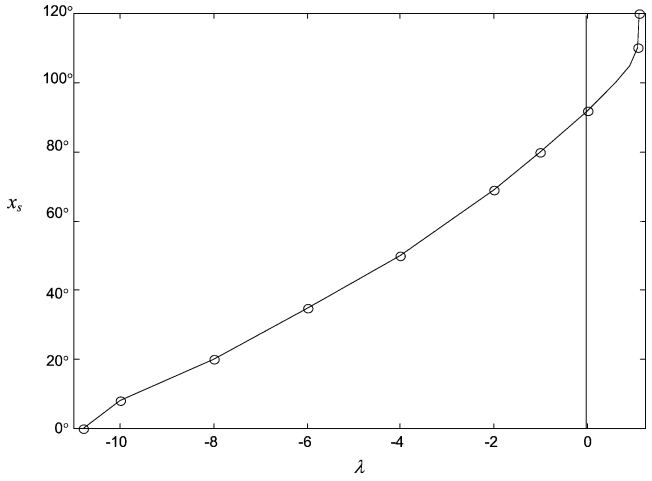

Fig. 13. Variation of the boundary layer separation point x_s with λ for $K = 1$ and $Pr = 7$.

next to the sphere to move downwards under the action of the buoyancy forces (see Merkin [21]). This is an unstable situation and whether a boundary layer can exist at all on the sphere for a value of $\lambda = \lambda_K (< 0)$ is still an open question.

We can show, following Merkin [21], that the separation of the boundary layer will not occur for $\lambda > \frac{9}{8}$. We see that for $y = 0$ Eqs. (15) and (16) give

$$(1+K)\left(\frac{\partial^3 \psi}{\partial y^3}\right)_{y=0} + \left(\lambda + \frac{9}{4}\cos x\right)\sin^2 x = 0 \qquad (41)$$

Although $(\partial^2\psi/\partial y^2)_{y=0} = 0$ at $x = x_s$, the streamwise velocity component $u = (1/r)\partial\psi/\partial y$ will be positive near $y = 0$ and so $(\partial^3\psi/\partial y^3)_{y=0} \geqslant 0$ at $x = x_s$. We thus have $(\lambda + (9/4)\cos x)\sin^2 x \leqslant 0$, which cannot hold in the range $0 \leqslant x \leqslant 120°$ for $\lambda > 9/8$.

5. Conclusions

In this paper we have theoretically studied the problem of steady mixed convection boundary layer flow over a sphere with constant temperature, which is immersed in a micropolar fluid. Solutions of the transformed non-similar boundary layer equations are obtained numerically using the Keller-box method along with the Newton's linearization technique. We have sought to determine how the material parameter K, the mixed convection parameter λ and the Prandtl number Pr affect the flow and heat transfer characteristics as well as the position x_s of the boundary layer separation. From this study we can draw the following conclusions:

- an increase in the values of the material parameter K leads to an increase of the local skin friction coefficient C_f and a decrease of the local heat transfer coefficient $Q_w(x)$
- an increase in the value of Pr leads to a decrease of the local skin friction coefficient C_f and an increase of the local heat transfer coefficient $Q_w(x)$
- an increase in the value of K leads to an increase of the value of λ (< 0) below which a boundary layer solution is not possible and to an increase of the value of λ (> 0) which first gives no separation

Acknowledgements

The authors wish to thank the Ibn Sina Institute for Fundamental Science Studies of Universiti Teknologi Malaysia for financial support and for giving one of the authors (IP) the chance to visit this University. The authors also thank the referees for the valuable comments.

References

[1] A.C. Eringen, Theory of micropolar fluids, J. Math. Mech. 16 (1966) 1–18.
[2] A.C. Eringen, Theory of thermomicrofluids, J. Math. Anal. Appl. 38 (1972) 480–496.
[3] T. Ariman, M.A. Turk, N.D. Sylvester, Microcontinuum fluid mechanics—A review, Internat. J. Engng. Sci. 11 (1973) 905–930.
[4] R.S.R. Gorla, Mixed convection in a micropolar fluid from a vertical surface with uniform heat flux, Internat. J. Engng. Sci. 30 (1992) 349–358.
[5] R.S.R. Gorla, A. Slaouti, H.S. Takhar, Free convection in micropolar fluids over a uniformly heated vertical plate, Internat. J. Numer. Methods Heat Fluid Flow 8 (1998) 504–518.
[6] S. Bhattacharyya, I. Pop, Free convection from cylinders of elliptic cross section in micropolar fluids, Internat. J. Engng. Sci. 34 (1996) 1301–1310.
[7] M.A. Hossain, M.K. Chowdhury, Mixed convection flow of micropolar fluid over an isothermal plate with variable spin gradient viscosity, Acta Mech. 131 (1998) 139–151.
[8] D.A.S. Rees, A.P. Bassom, The Blasius boundary-layer flow of a micropolar fluid, Internat. J. Engng. Sci. 34 (1996) 113–124.
[9] D.A.S. Rees, I. Pop, Free convection boundary-layer flow of a micropolar fluid from a vertical flat plate, IMA J. Appl. Math. 61 (1998) 179–197.
[10] M.A. Hossain, M.K. Chowdhury, H.S. Takhar, Mixed convection flow of micropolar fluids with variable spin-gradient viscosity along a vertical flat plate, Internat. J. Theoretical Appl. Fluid Mech. 1 (1995) 64–77.
[11] M.A. Hossain, M.K. Chowdhury, R.S.R. Gorla, Free convection flow of thermomicropolar fluid along a vertical plate with nonuniform surface temperature and surface heat flux, Internat. J. Numer. Heat Fluid Flow 9 (1999) 568–585.
[12] M.A. Hossain, M.K. Chowdhury, R.S.R. Gorla, Natural convection of thermomicropolar fluid from an isothermal surface inclined at a small angle to the horizontal, Internat. J. Numer. Heat Fluid Flow 9 (2000) 814–832.
[13] R. Nazar, N. Amin, I. Pop, Free convection boundary layer about a horizontal circular cylinder in a micropolar fluid, in: Proc. 12th Internat. Heat Transfer Conference, Grenoble, France, Vol. 2, August 2002, pp. 525–530.
[14] R. Nazar, N. Amin, I. Pop, Free convection boundary layer flow on a horizontal circular cylinder with constant surface heat flux in a micropolar fluid, Internat. J. Appl. Mech. Engng. 7 (2002) 409–431.
[15] R. Nazar, N. Amin, T. Grosan, I. Pop, Free convection boundary layer on an isothermal sphere in a micropolar fluid, Internat. Comm. Heat Mass Transfer 29 (2002) 377–386.
[16] F.-S. Lien, C.-C. Chen, Mixed convection of micropolar fluid about a sphere with blowing and suction, Internat. J. Engng. Sci. 24 (1987) 775–784.
[17] T.Y. Wang, C. Kleinstreuer, Thermal convection of micropolar fluids past two-dimensional or axisymmetric bodies with suction/injection, Internat. J. Engng Sci. 26 (1988) 1267–1277.
[18] T. Cebeci, P. Bradshaw, Physical and Computational Aspects of Convective Heat Transfer, Springer-Verlag, New York, 1984.
[19] R. Nazar, N. Amin, I. Pop, On the mixed convection boundary layer flow about an isothermal sphere, Arabian J. Sci. Engng., accepted.
[20] T. Chiang, A. Ossin, C.L. Tien, Laminar free convection from a sphere, J. Heat Transfer 86C (1964) 537–542.
[21] J.H. Merkin, Mixed convection from a horizontal circular cylinder, Internat. J. Heat Mass Transfer 20 (1977) 73–77.